

FROM ELECTRIC TO ACOUSTIC VIOLIN: DIGITAL SYNTHESIS AND EMULATION

P Gaydecki School of Electrical and Electronic Engineering, University of Manchester, UK
A Barton School of Electrical and Electronic Engineering, University of Manchester, UK
SF Minhas School of Electrical and Electronic Engineering, University of Manchester, UK
S Ismail School of Electrical and Electronic Engineering, University of Manchester, UK

1 INTRODUCTION

Real-time signal processing based on both general purpose microprocessors and fast digital signal processors (DSPs) is a technique that emerged over twenty years ago, and is now widely considered one of the fastest growing application areas in the field of digital technology. Typically, the analogue waveform is first digitized by an analogue to digital converter (ADC), and the binary values are transmitted to a DSP device that performs a real-time convolution operation in discrete space using either a finite impulse response (FIR) or infinite impulse response (IIR) algorithm. The processed data are then sent to a digital to analogue converter (DAC) that outputs a filtered analogue signal.

Here, we describe a highly integrated stand-alone system, based on DSP technology, which has been developed to process the raw electrical output from an electric violin to produce an output signal which, when fed to an amplifier and loudspeaker, approximates closely the timbre of an acoustic instrument. The system comprises a very high impedance preamplifier, a 24-bit sigma delta codec and a digital signal processor (DSP) operating at 590 million multiplications-accumulations per second (MMACs). The device holds in its memory up to fifty far-field impulse responses of wooden instruments, any one of which may be convolved in real-time with the input signal to synthesize the modified output signal. This first stage convolution is realized as an FIR structure. In addition, the device incorporates a parametric equalizer, blender, reverberation unit and a gain adjustment function. The user interface includes a set of navigator-style buttons and a simple display screen. The device may be connected to a computer or tablet and controlled from a separate software package. Preliminary trials with a professional violinist have confirmed that the system improves significantly the tonal quality of the raw string force signal.

It is important to recognize however, the limitations of this approach to electric violin enhancement. The sound radiation pattern emanating from a wooden body is spatially dependent: for example, the frequency response from the side of the instrument is quite distinct from the same measurement taken from the front or rear sound plates. The system described here only manipulates the far-field response. Perhaps most important, the hardware does not provide any form of feedback to the player from the string to bow.

2 BACKGROUND PRINCIPLES

2.1 Violin characterisation and perception

In all stringed instruments, the player directly controls only the motion of the strings. The vibrating strings exert forces on the instrument bridge, which cause the body to vibrate. The body vibration radiates sound, and in the process the string's waveform is modified by the pattern of body resonances. The musical qualities, and hence the value, of a particular instrument are determined by this pattern of resonances. This much is agreed by musicians, instrument-makers and scientists. However, much work is still required to establish, from a scientific perspective, the explicit relationships between these resonance characteristics and the perceptions of musical performers

and listeners. This situation limits severely the interpretability of acoustical data by scientists, musicians and instrument-makers, who are forced to fall back on anecdotal understanding of musical sound production by, and perception of, stringed instruments. Data are needed concerning the degree to which different physical characteristics of stringed instrument sounds are operational in the perceptions of performers and listeners, so that we can begin to understand the perceptual mechanisms that mediate sound production, and to predict the perceptual effect of changes in features of instrument construction and design. Without it, the ability to evaluate the bases for judgements about the musical acceptability of different instruments remains strictly hypothetical and pre-scientific. In some regard, the device described here offers a potential route forward, not only in relation to improvement in sound quality of body-less violins, but also in the area of psychoacoustics.

Enough is known about stringed-instrument body vibration response to ensure that adequate physical models can be developed; furthermore, recently-developed DSP techniques provide the means for resonant characteristics to be simulated and changed in real time. Such tools can facilitate comprehensive empirical investigations of the relationships between physical and perceptual dimensions of musical sound. These investigations could illuminate the cognitive and perceptual mechanisms that underlie the capacity to identify and discriminate between musical sounds, and would clarify for musicians and instrument-makers the musical-perceptual significance of a wide range of physical instrument parameters.

2.2 The violin as a linear system

The body of a violin is, to a very close level of approximation, a linear system. Although its properties do alter over time (as the wood, varnish and adhesives age), these changes only become significant over years. Within any reasonable time frame, the body manifests the property of temporal invariance. Hence if the body is tapped at a particular position using an instrumented hammer, the sound that it produces will always retain the same spectral characteristics (although the amplitude may vary, depending on the strength of the strike). Non-linearities are often introduced during performance, but these are player-dependent and confined to manner in which the bow moves over the string, not the body. Although the near-field impulse response is spatially variable, in the far-field these variations are less significant; it the far-field which is of interest in this case.

The characterization of a violin body as a linear system is pivotal since it allows the vibration behaviour to be characterized by the standard methods of linear acoustics, as has been explored by many researchers^{1,2,3}. The most extensive attempts to date to use the linear model to explore the resonance characteristics of real stringed instruments have been conducted by Jansson and Dönnwald^{4,5,6}. Dönnwald measured resonance characteristics of about 700 violins and found that certain resonance features (such as the presence of strong resonances in the region 190-650 Hz and 1300-4200 Hz relative to resonances in the regions 650-1300 Hz and 4200-6500 Hz) were characteristic of 'Old Italian' instruments; he concluded that these features were significant in determining the acceptability of violin sounds, but conducted no empirical research to explore or support the perceptual validity of this claim.

When performing on stage, violinists often use a microphone to amplify the sound from the violin; this has its disadvantages. The voice of the instrument is often not reproduced with fidelity since the microphone is in the near-field radiation zone of the transfer function. Additionally, interference is often introduced. From a pragmatic perspective, acoustic instruments are often very expensive – a typical Stradivarius will cost upwards of \$5M.

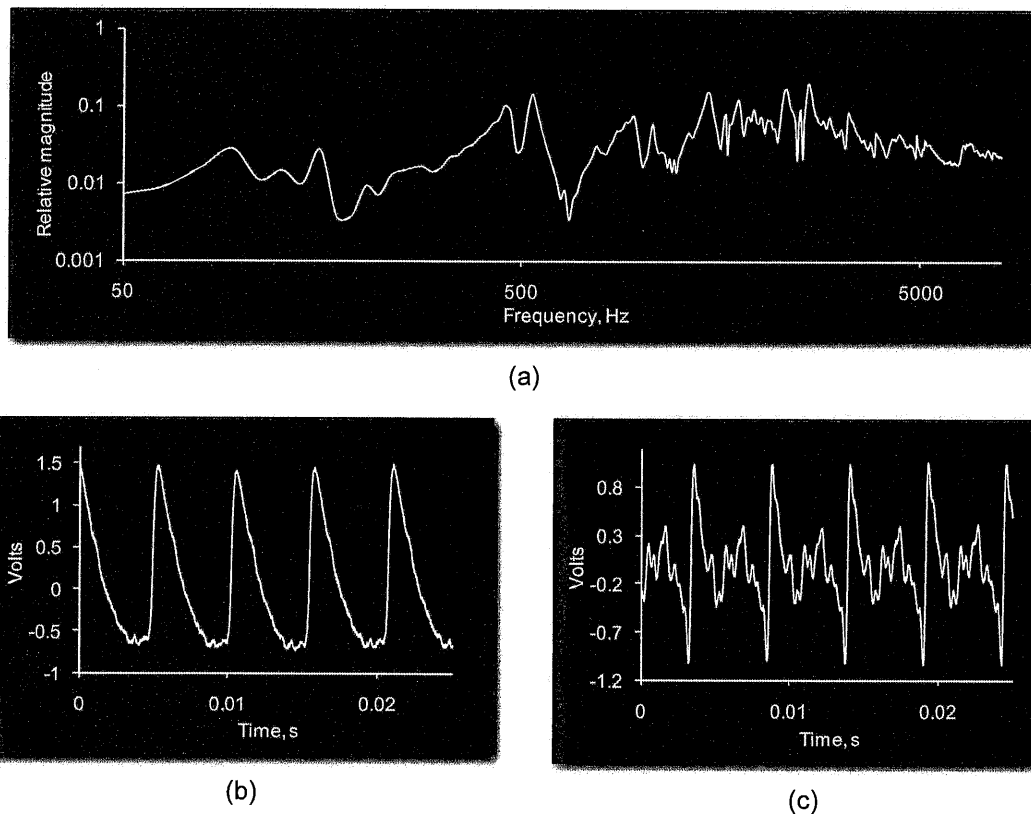


Figure 1. (a) Typical violin body frequency response; (b) force signal on bridge of violin; (c) force signal on bridge of violin mediated by body frequency response.

An approximate violin bridge/body impulse response can be obtained by tapping the bridge with a small instrumented hammer and using a microphone and an ADC to record the signal. This impulse response is then processed with an FFT algorithm to obtain the frequency response. A typical violin body frequency response is shown in Figure 1a. The force signal from just a string may be obtained using miniature accelerometers mounted on the bridge; a typical signal is shown in Figure 1b. This is then processed digitally with the bridge/body filter to synthesize a convincing violin sound; the resulting waveform⁷ appears in Figure 1c. An accurate measurement of the impulse response is technically challenging, and many publications have discussed this subject^{8,9}.

2.3 Basic DSP filter theory

The real-time filtering system employs a combination of both finite impulse response (FIR) and infinite impulse response (IIR) filters to affect the processing of the input force signal. Specifically, an FIR algorithm convolves the incoming signal with the body impulse response, and an IIR structure is used for both the parametric equalizer and the reverberation stage. In general, the convolution integral in continuous space is expressed as:

$$y(t) = \int_{-\infty}^{\infty} h(\tau)x(t-\tau)d\tau \quad (1)$$

where $y(t)$ is the output (filtered) signal, $x(t)$ is the incoming signal, τ is the time-shift operator and $h(\tau)$ is the impulse response of the filter. In discrete space, this equation may be implemented using either an FIR or IIR solution. In the former case, the infinite response is truncated, which yields an expression of the form:

$$y[n] = \sum_{k=0}^M h[k]x[n-k] \quad (2)$$

with the z -transform of the impulse response, ie the *transfer function* $H(z)$, being given by:

$$H(z) = \frac{Y(z)}{X(z)} = \sum_{n=0}^{\infty} h[n]z^{-n} \quad (3)$$

In contrast, IIR filters rely on recurrence formulae, where the output signal is given by:

$$y[n] = \sum_{k=0}^N a[k]x[n-k] - \sum_{k=1}^M b[k]y[n-k] \quad (4)$$

and the transfer function is given by:

$$H(z) = \frac{a[0] + a[1]z^{-1} + \dots + a[M]z^{-M}}{1 + b[1]z^{-1} + \dots + b[N]z^{-N}} = \frac{\sum_{m=0}^M a[m]z^{-m}}{1 + \sum_{n=1}^N b[n]z^{-n}} \quad (5)$$

There are important consequences associated with these two approaches to filtering; one of the most important criteria in assessing the performance of a filter is its stability. As Equations (2) and (3) show, FIR filters are unconditionally stable since there is no feedback in the convolution process. In contrast, IIR filters always feed back a fraction of the output signal, which necessitates careful attention to design if stability is to be ensured. This may be viewed another way: Equation (5) shows that the transfer function is the ratio of two polynomials in ascending negative powers of z . Thus high-order polynomials are associated with very small denominator terms and hence the risk of an ill-conditioned division. It is for this reason that IIR filters are sensitive to the word-length of the DSP device. In general, the higher the order of the filter, the greater the risk of instability, so high-order IIR filters are often designed by cascading together several low-order sections.

2.4 Parametric equalization

The parametric equalizer is realized as a parallel bank of twenty narrowband IIR filters with adjustable gains and bandwidths. Each filter is equivalent to an analogue LCR system shown in Figure 2a. In all cases, the resonant point of the filters is given by

$$\Omega = \frac{1}{\sqrt{LC}} \quad (6)$$

It is from Ω that the pre-warp frequency Ω^* is obtained using the relationship

$$\Omega^* = \frac{2}{T} \tan(\Omega T / 2) \quad (7)$$

This is necessary to correct for the low frequency mismatch between the continuous frequency variable Ω and its discrete equivalent ω . The (Laplace) transfer function is given by

$$H(s) = \frac{sRC}{s^2LC + sRC + 1} \quad (8)$$

The BZT substitution gives

$$H(z) = \frac{\frac{2}{T}RC \left[\frac{1-z^{-1}}{1+z^{-1}} \right]}{\left(\frac{2}{T} \right)^2 LC \left[\frac{1-z^{-1}}{1+z^{-1}} \right]^2 + \frac{2}{T}RC \left[\frac{1-z^{-1}}{1+z^{-1}} \right] + 1} \quad (9)$$

Using the identities

$$a = 2\frac{RC}{T} \quad b = \left(\frac{2}{T\Omega^*}\right)^2 \quad (10)$$

then substitution yields

$$H(z) = \frac{a - az^{-2}}{(a+b+1) + (2-2b)z^{-1} + (b-a+1)z^{-2}} \quad (11)$$

For the purposes of filter gain normalisation, the constant term in the denominator must be unity; to simplify the algebra, we make use of the following identities:

$$\varepsilon_0 = \frac{a}{(a+b+1)} \quad \varepsilon_1 = \frac{(2-2b)}{(a+b+1)} \quad \varepsilon_2 = \frac{(b-a+1)}{(a+b+1)} \quad (12)$$

Equation (11) therefore reduces to

$$H(z) = \frac{\varepsilon_0(1-z^{-2})}{1 + \varepsilon_1 z^{-1} + \varepsilon_2 z^{-2}} \quad (13)$$

Finally, the difference equation of the IIR filter is obtained directly from Equation 9.30, i.e.

$$y[n] = \varepsilon_0(x[n] - x[n-2]) - \varepsilon_1 y[n-1] - \varepsilon_2 y[n-2] \quad (14)$$

The centre frequency and bandwidth of each filter is determined by the coefficients ε_0 , ε_1 and ε_2 . Each filter also has an output gain parameter that the user adjusts via a slider control from the high level software. The complete equalizer is shown in Figure 2b, and the overlapping frequency responses in Figure 2c.

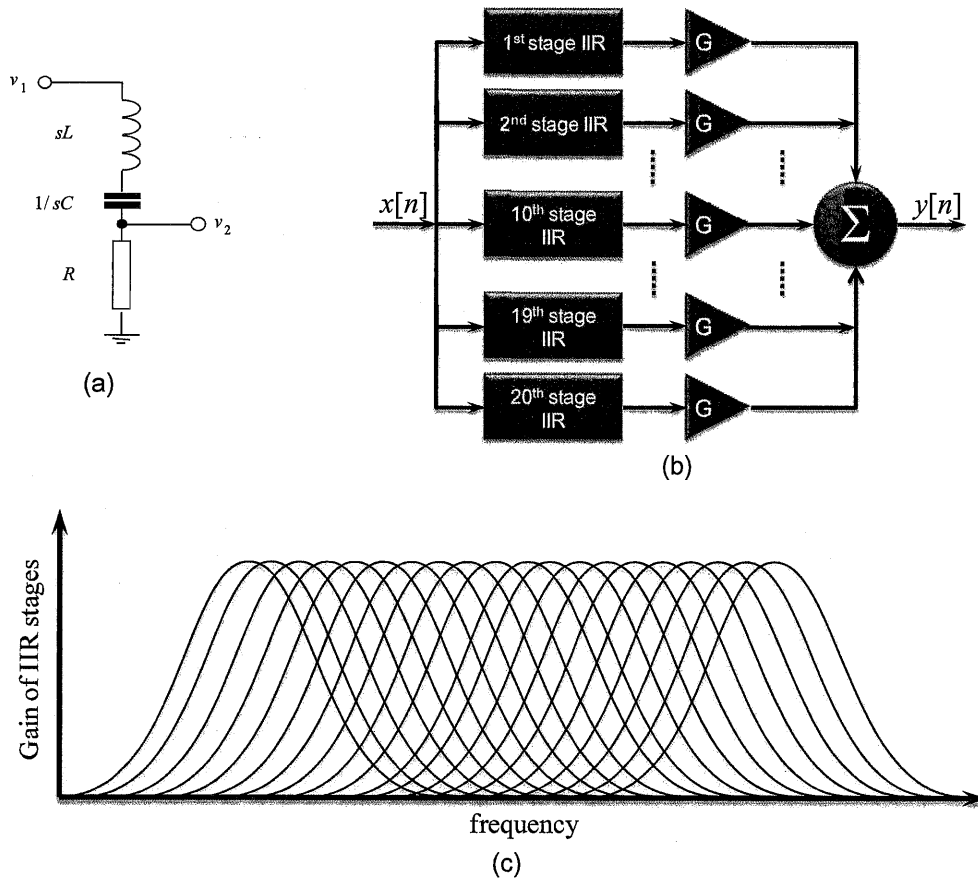


Figure 2. (a) Equivalent LCR filter; (b) 20-band IIR equalizer; (c) equalizer frequency response.

Reverberation stage

A reverberation stage has been included in the processing stream to enhance the warmth and spaciousness of the perceived sound output. The digital reverb algorithm used is adapted from a scheme first proposed by J. A. Moorer¹⁰, the concept of which is depicted in Figure 3a. The input signal is first fed to a bank of parallel comb filters (as above), but modified to accommodate the selective high frequency absorption from the reflecting surfaces. These comb filters are intended to replicate the effects of multiple reflecting surfaces found in most physical enclosed spaces. The outputs of the parallel filters are then summed and fed to an all-pass filter, which has a flat frequency response but randomizes the phases of the various echoes. Finally, the direct path signal is added to the indirect (echo) signals.

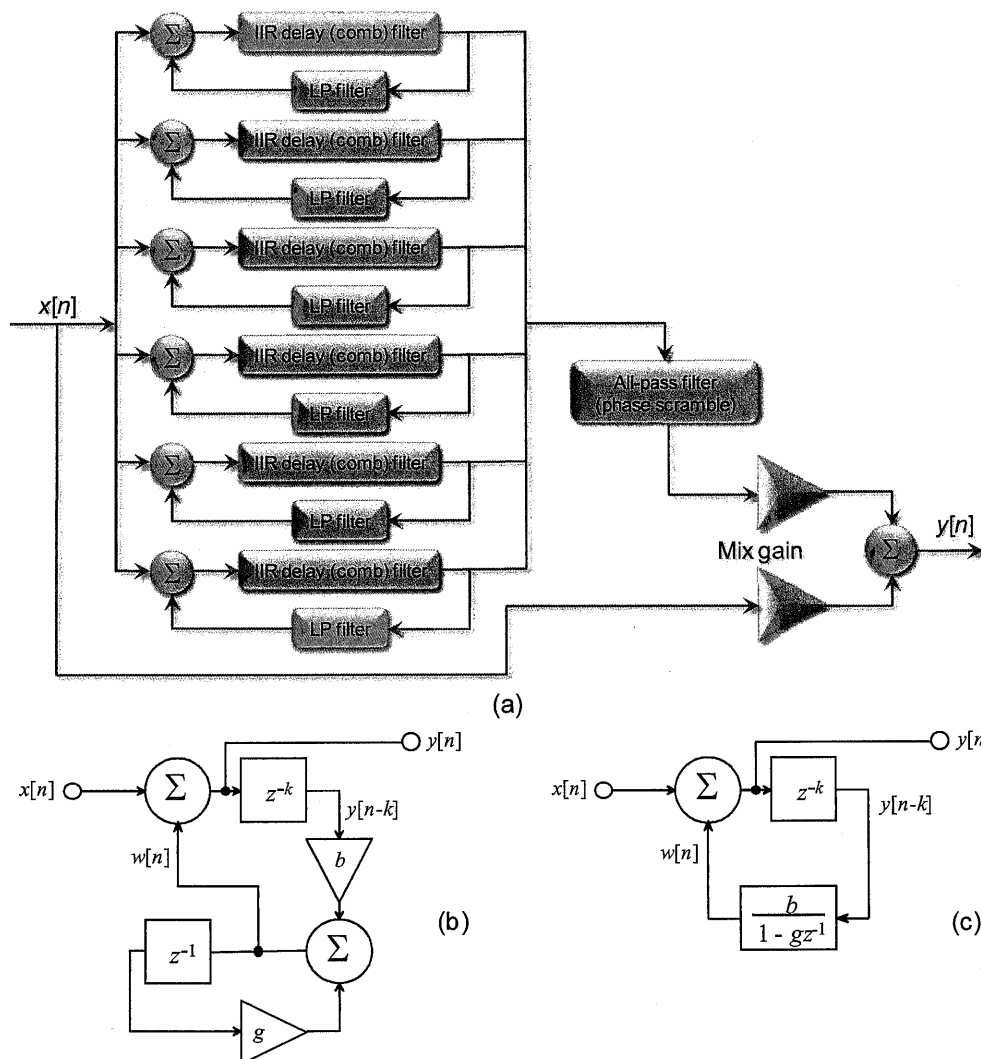


Figure 3. Reverberation unit. (a) complete system; (b) IIR comb filter with low pass feedback; (c) simplified representation of (b).

Each comb filter, together with its single pole low pass feedback filter, is shown in Figures 3b and 3c. The total transfer function is:

$$H(z) = \frac{1}{1 - \left(\frac{b}{1 - gz^{-1}} \right) z^{-k}} = \frac{1 - gz^{-1}}{1 - gz^{-1} - bz^{-k}} \quad (15)$$

The reverberation difference equation is therefore:

$$y[n] = x[n] - gx[n-1] + gy[n-1] + by[n-k] \quad (16)$$

The final component of the reverberation algorithm is the all-pass filter, which disrupts the phases of the various signals. The inclusion of the all-pass filter is appropriate since multiple reflections cause randomisation of the phases of the signal's harmonics. The transfer function of the all-pass filter is:

$$H(z) = \frac{a + z^{-m}}{1 + az^{-m}} \quad (17)$$

In this case, the value selected for a is 0.7 and m is equal to 10 milliseconds (typical for room acoustics).

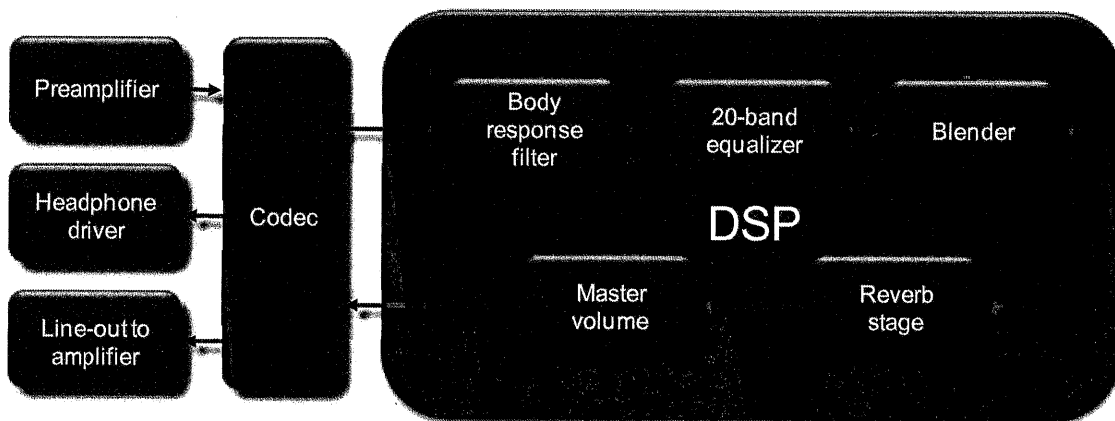


Figure 4. Main system components and signal processing chain.

3 HARDWARE SYSTEM AND SIGNAL PROCESSING CHAIN

A hardware system has been designed to perform the operations described above in real time. The output from the string pickup (normally a piezo-electric transducer) is fed to a high-impedance ($5\text{ M}\Omega$) gain-switchable preamplifier and then to the analogue-to-digital converter section of a 24-bit codec sampling at 50 kHz. The output from the codec is then fed to the DSP device with a processing power of 590 MMACs, which performs all of the main-stage processing, i.e. body impulse response convolution, parametric equalization, blending (dry/wet mixing), reverberation and final volume control. The processing chain is depicted in Figure 4. After processing, the output signal is fed back to the digital-to-analogue section of the codec and from there to appropriate buffers to drive both high power audio amplifiers and headphones. Other sub-systems include a display, keypad and interface to allow the unit to be connected to and programmed by a computer. The final device is shown in Figure 5. Convolution of signal with a long-duration impulse response is a compute-intensive operation. In the case of signals sampled within the audio band, it places a severe constraint on the specifications of the DSP device which is selected to perform the task. In this case, for example, the impulse response comprises 4096 coefficients. With a sample rate of 50 kHz, this alone represents a processing burden of 204.8 MMACs. In addition, the processing core must also accommodate the twenty IIR filters in the equalizer, the seven comb / low-pass filters and phase scrambler of the reverb unit, a master gain and the blender function. Modern DSP devices achieve the speeds required with the use of Harvard architecture, hardware multipliers and enhanced filter coprocessors, which are optimized to perform seamless multiplication and accumulation. Typically, such systems perform convolution at close to or equal 100% efficiency (i.e. two MMACs per clock cycle when using both the DSP core and the coprocessor).

4 CONCLUSION

A prototype system has been described that is intended to approximate, in real-time, the far-field impulse response of an acoustic (wooden) violin. It comprises a high-speed DSP core and codec in combination with software that convolves the incoming signal with a measured far-field radiative response. Other features include a user-controlled parametric equalizer, reverberation unit and blender function. Preliminary tests suggest that the device may enhance significantly the voice of an electric instrument; additionally, it represents an ideal research tool due to its flexibility and the ease with which the entire convolution operation may be reconfigured.

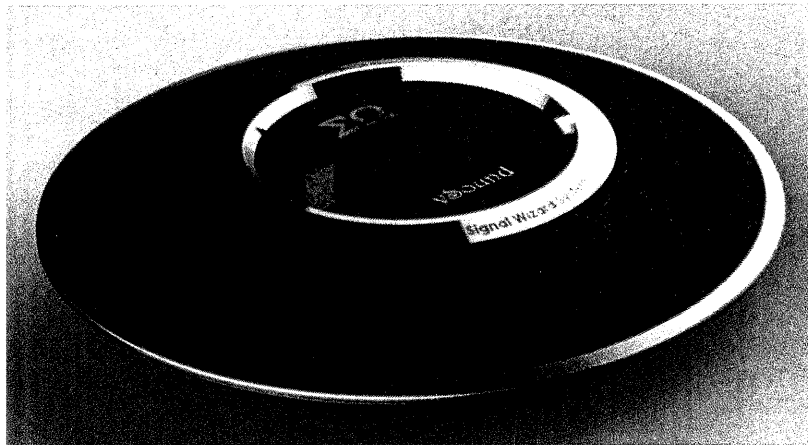


Figure 5. Complete device showing display screen and navigator buttons.

5 REFERENCES

1. L. Cremer, *The physics of the violin*: MIT Press, Cambridge, Mass. (1985)
2. K. D. Marshall, Modal analysis of a violin: *J. Acoust. Soc. Amer.* 77, 695–709 (1985)
3. C. M. Hutchins, *Research papers in violin acoustics 1975–1993*: Acoustical Society of America, Woodbury NY. (1997)
4. E. Jansson and B. Niewczyk, On the acoustics of the violin: bridge or body hill: *CAS Journal Series* 2(3) 23–27 (1999)
5. E. Jansson, Admittance measurements of 25 high quality violins: *Acustica - Acta Acustica* 83 337–341 (1997)
6. H. Dönnwald, Deduction of objective quality parameters on old and new violins: *J. Catgut Acoust. Soc. Series* 2(1) 1–5 (1991)
7. P. Gaydecki J. Woodhouse and I. Cross, Advances in audio signal enhancement and stringed instrument emulation using real-time DSP Proc. *Forum Acusticum Sevilla 2002* (on CD; ISBN: 84-87985-06-8) (2002)
8. P. Cook and D. Trueman, A database of measured musical instrument body radiation impulse responses, and computer applications for exploring and utilizing the measured filter functions, *Proc. Int. Symp. Musical Acoust.* (Acoustical Society of America, Woodbury, NY), 303–308 (1998)
9. C. Fritz, I. Cross, B. Moore and J. Woodhouse, Perceptual thresholds for detecting modifications applied to the acoustical properties of a violin, *J. Acoust. Soc. Am.* 122, 3640–3650 (2007)
10. J. Moorer, About this Reverberation Business, *Computer Music Journal* 3(2):13–28 (1979)